# Temperature and Pressure Dependence of the Rate Constants of the Reaction of $NO_3$ Radical with $CH_3SCH_3$

**Yukio Nakano* and Takashi Ishiwata**

*Faculty of Information Sciences, Hiroshima City University, Hiroshima 731-3194, Japan*

**Simone Aloisio**

*California State University Channel Islands, One University Drive, Camarillo, California 93012*

**Masahiro Kawasaki**

*Department of Molecule Engineering, Kyoto University, Kyoto 615-8510, Japan*

*Received: February 27, 2006; In Final Form: April 11, 2006*

The reaction of nitrate radical with dimethyl sulfide was studied with cavity ring-down spectroscopy in 20−200 Torr of $N_2$ diluent in the temperature range of 283−318 K. The rate constant for this reaction, $k_1$, is found to be temperature dependent and pressure independent: $k_1 = 4.5^{+4.0}_{-2.8} \times 10^{-13} \exp[(310 \pm 220)/T]$ cm$^3$ molecule$^{-1}$ s$^{-1}$. The uncertainties are two standard deviations from regression analyses. The present rate constants are in good agreement with those reported by Daykin and Wine (*Int. J. Chem. Kinet.* **1990**, *22*, 1083) and may be used in the atmospheric model calculation. Theoretical calculations were carried out to verify the existence of an intermediate complex.

## 1. Introduction

Dimethyl sulfide (DMS), the largest natural source of atmospheric sulfur, is produced by phytoplankton in the oceans and is released into the atmosphere.[1−5] When DMS is oxidized in the atmosphere, the organic sulfur species become hygroscopic and may form condensation nuclei, leading to the production of aerosols and possibly clouds. Thus, the oxidation of DMS is of particular importance to the production of atmospheric aerosols, and hence to Earth's radiation balance and climate system.[6] The effects of aerosols and clouds remain as the largest uncertainty in climate forecasting today.[7] DMS has been considered to be mainly oxidized by reaction with hydroxyl (OH) radicals during the daytime.[8−11] At night, DMS is considered to be mainly oxidized by nitrate radical ($NO_3$) via the following reaction, because OH radical is absent in the atmosphere.[12−14]

$$NO_3 + CH_3SCH_3 \rightarrow CH_3SCH_2 + HNO_3 \qquad (1)$$

$NO_3$ radical is considered to be one of the most important oxidizer, especially in urban areas, because $NO_3$ is formed by the reaction of $NO_2$ with $O_3$.[15] Solar photolysis of $NO_3$ and the reaction with NO suppress the concentration of $NO_3$ at the daytime. Because of this, the mixing ratio of $NO_3$ peaks at nighttime. In the marine boundary, the concentration of $NO_3$ rises up to 10 ppt during the night.[16]

The rate constant of the reaction of $NO_3$ radical with DMS has been measured by several methods as listed in Table 1.[17−22] Wallington et al. reported the rate constant to be $(0.75 \pm 0.05) \times 10^{-12}$ cm$^3$ molecule$^{-1}$ s$^{-1}$ in 50−400 Torr of He diluent,[19] and $(0.81 \pm 0.13) \times 10^{-12}$ cm$^3$ molecule$^{-1}$ s$^{-1}$ in 50−100 Torr of $N_2$ diluent.[20] Other works reported $k_1 \approx 1 \times 10^{-12}$ cm$^3$ molecule$^{-1}$ s$^{-1}$ under 0.5−4.5 Torr of He diluent and 20 Torr of $N_2$ diluent.[17,21] Most recently Daykin and Wine[22] reported $k_1 = (1.3 \pm 0.3) \times 10^{-12}$ cm$^3$ molecule$^{-1}$ s$^{-1}$ in 19−500 Torr of $N_2$ and air diluent. NASA/JPL[23] and IUPAC[24] recommendation values for the rate constant of $NO_3$ + DMS to use the atmospheric model calculation are $1.0 \times 10^{-12}$ and $1.1 \times 10^{-12}$ cm$^3$ molecule$^{-1}$ s$^{-1}$, respectively.

Dlugokencky and Howard[21] and Wallington et al.[20] reported a negative temperature dependence for the rate constant in the ranges 256−376 and 280−350 K, respectively. Those results may be an indication of the formation of a short-lived intermediate complex:

$$NO_3 + CH_3SCH_3 \rightleftarrows [(CH_3)_2S(ONO_2)]^{\ddagger} \qquad (1a)$$

$$\rightarrow [(CH_3)_2S(ONO_2)] \rightarrow CH_3SCH_2 + HNO_3 \qquad (1b)$$

Daykin and Wine[22] and Jensen et al.[25] observed a significant deuterium isotope effect ($k_H/k_D = 3.8$ at room temperature), showing that the rate-determining step involves C−H (or C−D) bond breakage. However contradicting to these studies, the rate constants at several temperatures reported by Tyndall et al. shows the rate constant is temperature independent: $(1.2 \pm 0.3) \times 10^{-12}$ at 278 K, $(0.99 \pm 0.35) \times 10^{-12}$ at 298 K, and $(1.00 \pm 0.25) \times 10^{-12}$ cm$^3$ molecule$^{-1}$ s$^{-1}$ at 318 K.[18]

The previously reported experimental data show that the rate constant is independent of total pressure over the range from 0.5 to 760 Torr. For example, Daykin and Wine suggested the pressure independence of the rate constants in the rage of the total pressure of 19−500/$N_2$ or Air.[22]

In this work, we have reexamined the temperature and pressure dependence of the rate constant for $NO_3$ + DMS using cavity ring-down spectroscopy, which is known as a high sensitive absorption technique. The low detection limit achieved

* Corresponding author. E-mail: yukio_n@im.hiroshima-cu.ac.jp. Fax: +81-82-830-1825.

10.1021/jp0612230 CCC: $33.50 
Published on Web 05/18/2006

**TABLE 1: Rate Constants of $NO_3$ + DMS at Room Temperature**

| experimental technique | pressure (Torr)/diluent gas | $k_1$ ($10^{-12}$ cm$^3$ molecule$^{-1}$ s$^{-1}$) | ref |
|---|---|---|---|
| relative rate method | 735/air | $0.99 \pm 0.02^a$ | 17, 24 |
| molecular modulation | 20/$N_2$ | $1.0 \pm 0.2$ | 18 |
| flash photolysis with visible absorption | 50−400/He | $0.75 \pm 0.05$ | 19 |
| flash photolysis with visible absorption | 50−100/$N_2$ | $0.81 \pm 0.13$ | 20 |
| flow tube with laser-induced fluorescence | 0.5−4.5/He | $1.05 \pm 0.13$ | 21 |
| laser flash photolysis with visible absorption | 19−500/$N_2$, Air | $1.3 \pm 0.3$ | 22 |
| laser flash photolysis with cavity ring-down spectroscopy | 20−200/$N_2$ | $1.28 \pm 0.06^b$ | this work |

[a] The measured rate coefficient ratio of $k(NO_3 + CH_3SCH_3)/k(NO_3 + trans\text{-}2\text{-butene}) = 2.55 \pm 0.05$ is placed on an absolute basis by use of a rate coefficient of $k(NO_3 + trans\text{-}2\text{-butene}) = 3.89 \times 10^{-13}$ cm$^3$ molecule$^{-1}$ s$^{-1}$. [b] As mentioned in the text, the rate constant shows no pressure dependence. Thus, we adopte the rate constant deterined in 100 Torr of $N_2$ diluent.

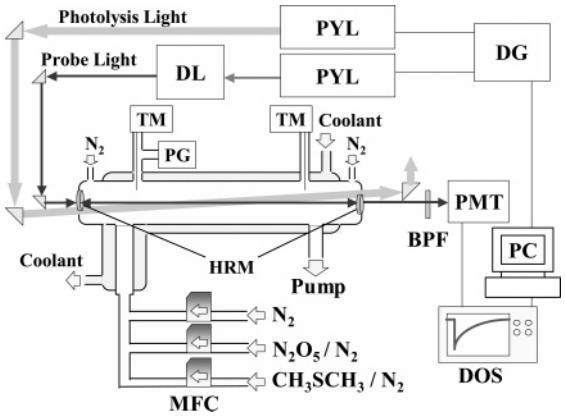


**Figure 1.** Experimental apparatus of cavity ring-down spectroscopy for the measurement of the reaction of $NO_3$ with DMS (HRM, high reflective mirror; PYL, pulsed $Nd^{3+}$:YAG laser; DL, dye laser; DG, delay generator; DOS, digital oscilloscope; PMT, photomultiplier tube; BPF, band-pass filter; MFC, mass flow controller; TM, thermometer; PG, pressure gauge).

by using the cavity ring-down spectroscopy technique allows us to keep radicals concentrations as low, hence reducing the complications from radical−radical reactions.

## 2. Experimental Section

Our cavity ring-down spectroscopy apparatus is shown in Figure 1 and similar to the previously reported one.[26] Two pulsed lasers were employed. A $Nd^{3+}$:YAG laser (Continuum Co., Surelite II) was used to photolyze nitrogen pentoxide ($N_2O_5$) at 266 nm to generate $NO_3$ radicals. A dye laser (Sirah Co., Cobra-Stretch; DCM Dye) pumped by the 532 nm output of a $Nd^{3+}$:YAG laser (Continuum Co., Surelite I) was used to probe the concentration of $NO_3$. After the photolysis laser beam traversed a reaction cell nearly collinear to the axis of the ring-down cavity, the probe laser beam was injected through one of two high-reflectivity mirrors which made up the ring-down cavity. The mirrors (Research Electro Optics) had a reflectivity of 0.9994 (correspond to the 5.6 $\mu$s of cavity ring-down time for vacuum) at 662.0 nm, a diameter of 7.75 mm, and a radius of curvature of 1 m and were mounted 1.04 m apart. Light leaking from one of the mirrors of the ring-down cavity was detected by a photomultiplier tube (Hamamatsu Photonics Co., R928) through a broad band-pass filter (656 nm, fwhm 10 nm). The decay of the light intensity was recorded using a digital oscilloscope (Tektronix TDS430A) and transferred to a personal computer. The decay of the light intensity is given by equation,

$$I(t) = I_0 \exp(-t/\tau) = I_0 \exp(-t/\tau_0 - \sigma nc(L_R/L)t) \quad (2)$$

where $I(t)$ is the intensity of light at time $t$. $\tau_0$ is the empty cavity ring-down time (5.6 $\mu$s at 662.0 nm). $L_R$ is the length of the reaction region (0.46 m) while $L$ is the cavity length (1.04 m); $\tau$ is the measured cavity ring-down time; $n$ and $\sigma$ are the concentration and absorption cross section of the species of interest; $c$ is the speed of light.

The reaction cell consisted of a Pyrex glass tube (21 mm i.d.), which was evacuated by an oil rotary pump. The volume of the detection region of reaction cell was 160 cm$^3$. The temperature of the gas flow region was controlled by circulation of a thermostated mixture of methanol and water and was controllable over the range from 283 to 318 K. The difference between the temperature of sample gases at the entrance and exit of the flow region was <1 K. The pressure in the cell was monitored by an absolute pressure gauge (MKS, Baratron). Gas flows were measured and regulated by mass flow controllers (KOFLOC, model 3660). A slow flow of nitrogen diluent gas was introduced at both ends of the ring-down cavity close to the mirrors to minimize deterioration caused by exposure to reactants and products. The total flow rate was kept constant at $1.0 \times 10^3$ cm$^3$ min$^{-1}$ (STP). Experiments were performed with 1−2 Hz laser operation. Hence the gas mixture in the detection region refreshed in 1−3 laser shots under the pressure conditions of these experiments.

$NO_3$ radicals were produced by the 266 nm photolysis (laser power is 10−80 mJ/pulse) of $N_2O_5$ ($0.3-3 \times 10^{15}$ molecules cm$^{-3}$) in 20−200 Torr of $N_2$ diluent.

$$N_2O_5 + h\nu(266\text{ nm}) \rightarrow NO_3 + NO_2 \quad (3)$$

The electronic transition $NO_3(B^2E' \leftarrow X^2A'_2)$ was monitored at 662.0 nm. The absorption of $NO_3$ was converted to the concentration by using the reported absorption cross section at 662 nm, $\sigma_{NO_3} = 2.0 \times 10^{-17}$ cm$^2$ molecule$^{-1}$.[23,27−29] Signal decays of $NO_3$ in the presence of excess DMS were used to provide kinetic data for the reaction of $NO_3$ + DMS. Since the reactions were carried out under pseudo-first-order conditions with DMS in excess, the $NO_3$ radical concentration does not have to be known with high accuracy.

$N_2O_5$ was synthesized by the method reported by Caeser and Goldfrank.[30] Highly concentrated nitric acid ($HNO_3$) contained in a glass flask was cooled to dry ice temperature. Ozone in an $O_2$ stream was passed through the flask and $P_2O_5$ was added. Evolved $N_2O_5$ gas with $N_2O_4$ was collected in a cold trap at dry ice temperature. The condensation was fractionated by vacuum distillation. Other reagents were obtained from commercial sources. DMS (99.0%) was subjected to repeated freeze−pump−thaw cycles before use. $N_2$ (>99.9995%) and He (>99.9999%) were used without further purification.

The mixtures of $N_2O_5$/buffer gas and DMS/buffer gas, prepared and stored in a glass bulb, were injected into the reaction cell using mass flow controllers. The concentrations of $N_2O_5$ and DMS in the reaction cell could be calculated by using the flow rates.

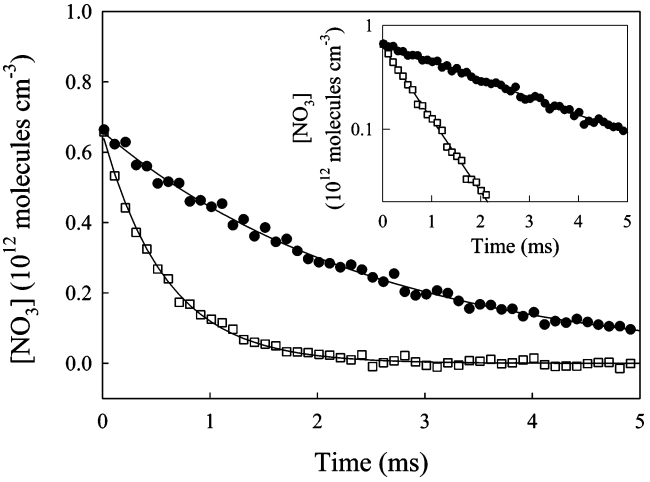


**Figure 2.** Pseudo-first-order decay profiles of $NO_3$ radical with [DMS] = 0 (closed circles) and [DMS] = $9.7 \times 10^{14}$ molecules $cm^{-3}$ (open squares) in 100 Torr of $N_2$ diluent at 298 K. The curve is a fit of eq 7 to the data.

## 3. Results and Discussion

**3.1. Experimental Study of the Reaction of $NO_3$ with DMS.** $NO_3$ was produced by the 266 nm photolysis of $N_2O_5$ at a total pressure of 100 Torr with $N_2$ diluent at temperatures of 298 K. Under these conditions, $NO_3$ was lost via the following reaction pathways.

$$NO_3 \rightarrow \text{diffusion and wall loss} \quad (4)$$

$$NO_3 + NO_3 \rightarrow \text{products} \quad (5)$$

$$NO_3 + NO_2 \rightarrow NO + NO_2 + O_2 \quad (6a)$$

$$NO_3 + NO_2 + M \rightarrow N_2O_5 + M \quad (6b)$$

As discussed in our previous work, the processes 5, 6a, and 6b do not contribute significantly to the consumption of $NO_3$, and process 4 is the dominant pathway for the consumption of $NO_3$.[31] Figure 2 shows a typical decay profile of $NO_3$ measured under these conditions ([$N_2O_5$] = $3 \times 10^{14}$ molecules $cm^{-3}$), in which the measured decay profile of $NO_3$ is well reproduced by a single-exponential decay curve:

$$[NO_3]_t = [NO_3]_0 \exp(-k' t) \quad (7)$$

where $[NO_3]_t$ and $[NO_3]_0$ are the concentrations of $NO_3$ at time $t = 0$ and $t$, respectively; $k'$ is the first-order rate constant for the loss of $NO_3$.

To determine the rate constant of $NO_3$ with DMS, temporal profiles of $NO_3$ were measured in the presence of excess DMS (up to $3.2 \times 10^{15}$ molecules $cm^{-3}$). Under these conditions, $NO_3$ radicals were lost via reactions 1 and 4 and a single-exponential decay is shown in Figure 2 for [$CH_3SCH_3$] = $9.7 \times 10^{14}$ molecules $cm^{-3}$. In eq 7, $k'$ is expressed by the following equation.

$$k' = k_1[DMS] + k_4 \quad (8)$$

The decay profiles of $NO_3$ were analyzed with the same procedure, and $k'$ was determined at several concentrations of DMS. Figure 3 shows $k'$ vs [DMS] in 100 Torr of $N_2$ diluent at 298 K. By considering the relationship of eq 8, a linear least-squares analysis gives $k_1 = (1.28 \pm 0.06) \times 10^{-12}$ $cm^3$ $molecule^{-1}$ $s^{-1}$. Uncertainty reported here is two standard deviations determined by the fitting method. The present value

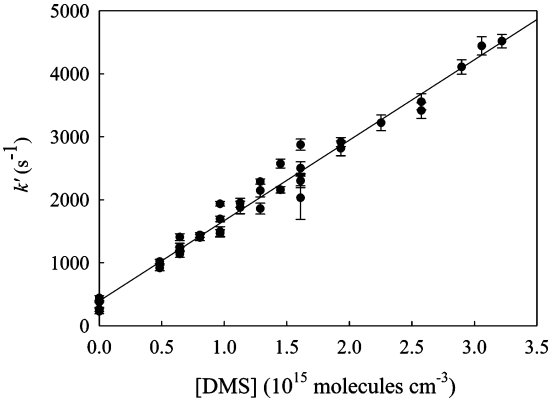


**Figure 3.** Plot of $k'$ vs concentration of DMS for data in 100 Torr of $N_2$ diluent at 298 K. The solid line is a linear least-squares fit to the data, where $k'$ stands for $k_1$[DMS] + $k_4$.

**TABLE 2: Rate Constants for $NO_3$ + DMS Observed at Various Pressures and Diluents (298 K)**

| total pressure (Torr)/diluent gas | $k_1$ ($10^{-12}$ $molecule^{-1}$ $cm^3$ $s^{-1}$) |
|---|---|
| 20/He | $1.22 \pm 0.09$ |
| 20/$N_2$ | $1.27 \pm 0.12$ |
| 50/$N_2$ | $1.29 \pm 0.10$ |
| 100/$N_2$ | $1.28 \pm 0.06$ |
| 200/$N_2$ | $1.33 \pm 0.18$ |

**TABLE 3: Temperature Dependence of the Rate Constants for $NO_3$ + DMS in 100 Torr of $N_2$ Diluent**

| temp (K) | $k_1$ ($10^{-12}$ $molecule^{-1}$ $cm^3$ $s^{-1}$) |
|---|---|
| 283 | $1.37 \pm 0.06$ |
| 293 | $1.30 \pm 0.04$ |
| 298 | $1.28 \pm 0.06$ |
| 308 | $1.24 \pm 0.08$ |
| 318 | $1.24 \pm 0.13$ |

is in excellent agreement with that reported in most recent work by Daykin and Wine,[22] and is close to those reported by Atkinson et al.,[17] Tyndall et al.,[18] and Dlugokencky et al.[21] These results are summarized in Table 1.

To test the pressure effect by a diluent gas, additional experiments were performed at 20 Torr of He diluent and at 20, 50, and 200 Torr of $N_2$ diluent. Consequently, we obtain $k_1 = (1.22 \pm 0.09) \times 10^{-12}$ in 20 Torr of He diluent, $(1.27 \pm 0.12) \times 10^{-12}$ in 20 Torr of $N_2$ diluent, $(1.29 \pm 0.10) \times 10^{-12}$ in 50 Torr and $(1.33 \pm 0.18) \times 10^{-12}$ $cm^3$ $molecule^{-1}$ $s^{-1}$ in 200 Torr. Uncertainties reported here are two standard deviations determined by the fitting method. These results are summarized in Table 2. These data are consistent within experimental error, therefore any pressure dependence that might exist is very slight. Therefore, our experimental results suggest that the rate constant for the reaction of $NO_3$ with DMS is pressure independent for the range of pressures and dileunt gases used here (20−200 Torr of He and $N_2$). These results agree with that reported by Daykin and Wine.[22] We conclude that the present value determined in 100 Torr of $N_2$ is appropriate for use in atmospheric models, because of no notable pressure dependence in the reaction rate constant.

To determine the temperature dependence in 100 Torr of $N_2$ diluent, $k_1$ was measured at various temperatures, 283−318 K. (Table 3 and Figure 4). Figure 4 shows the negative temperature dependence for the reaction of $NO_3$ with DMS. The tendency of the temperature dependence of the rate constant agrees with that reported by Dlugokencky and Howard,[21] and by Wallington et al.[20] A linear least-squares analysis of the present data with weighting by the inverse of dispersions for each data gives $k_1 = 4.5^{+4.0}_{-2.8} \times 10^{-13} \exp[(310 \pm 220)/T]$ $cm^3$ $molecule^{-1}$ $s^{-1}$.

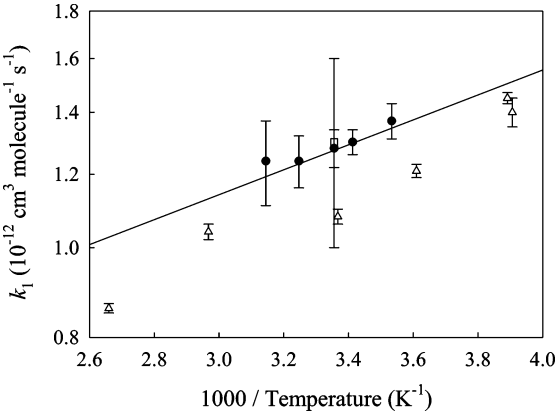


**Figure 4.** Temperature dependence of the rate constants of $NO_3$ + DMS in 100 Torr of $N_2$ diluent. Present work (closed circles), Dlugokecky et al. of ref 21 (open triangles) and Daykin and Wine of ref 22 (open squares).

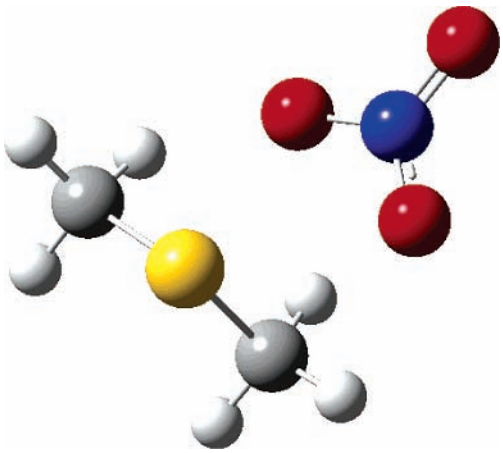

**Figure 5.** Calculated structure of the DMS−$NO_3$ complex.

Uncertainties reported here are two standard deviations determined by the fitting method. The negative activation energy ($E_a = -2.6 \pm 1.8$ kJ mol$^{-1}$) determined herein is consistent with that determined by Dlugokencky and Howard[21] ($E_a = -4.4 \pm 0.2$ kJ mol$^{-1}$) and Wallington et al.[20] ($E_a = -1.4 \pm 1.1$ kJ mol$^{-1}$) within experimental errors, The negative activation energy suggests that the reaction of $NO_3$ with DMS proceeds via an associated complex as shown reactions 1a and 1b.

**3.2. Theoretical Study of the Reaction of $NO_3$ with DMS.** Theoretical calculations were done to verify the existence of an intermediate complex as described in reaction 1. All calculations were performed using the GAUSSIAN 03[32] suite of programs. The results of the calculations presented here result from calculations performed at the B3LYP/6−311++(3df,3pd) level of theory[33,34] and the UMP2/6−311++(3df,3pd) level of theory.[35−37] We present geometry and energy results from our calculations of the lowest energy isomer found. It should be noted that frequency calculations have also been performed using the B3LYP method to verify that our structure is a true minimum and also to calculate the zero-point energy.

Figure 5 shows a diagram of the complex. The optimized geometry of the structure, calculated at using both the B3LYP/6-311++(3df,3pd) level of theory[38,39] and the UMP2/6−311++(3df,3pd) level of theory[40−42] is shown in the supplementary table and figure. Both levels of theory result in the calculation of a complex with a similar structure. The intermolecular bond distance between the sulfur atom and the nearest oxygen atom is calculated to be 2.206 Å using the UMP2 method and 2.383 Å using the B3LYP method. Another oxygen atom on the nitrate radical interacts slightly with a hydrogen atom of DMS. The intermolecular distance between these two atoms is calculated to be 2.698 Å using the UMP2 method and 2.586 Å using the B3LYP method. The angle formed between the C−S−C plane of the DMS and the nearest oxygen atom of nitrate radical is nearly perpendicular, and 85.0° at UMP2/6-311++(3df,3pd) level and 86.4° B3LYP/6-311++(3df,3pd) level of theory. The plane formed by the nitrate radical is nearly parallel to the S−C−H plane on the methyl side further from $NO_3$. All of the optimized geometric coordinates for the DMS−$NO_3$ complex are listed in supplementary Table S.1, and the structure is shown at three different angles in Figures S.1−S.4.

The two methods differ somewhat in their calculation of the well depth ($D_e$), however. At the UMP2 level of theory, the binding energy is 30.5 kJ mol$^{-1}$, while, using the B3LYP method, the well depth is calculated to be 59.0 kJ mol$^{-1}$. These are taken as a lower and upper limit for $D_e$ of this complex. The harmonic zero-point energy correction was calculated to be 13.0 kJ mol$^{-1}$, resulting in $D_0$ to be 17.6 kJ mol$^{-1}$ using the UMP2 method, and 46.0 kJ mol$^{-1}$ for the B3LYP method.

The reaction of OH with DMS is also known to form the similar complex as shown in the following reaction scheme.

$$OH + CH_3SCH_3 \rightleftarrows (CH_3)_2SOH \qquad (9)$$

The binding energy of complex formed between DMS and $NO_3$ determined here is similar in magnitude to the complex formed between DMS and OH, which has the same type of interaction between the S−O intermolecular coordinate. Using the same methods and basis sets, the binding energy ($D_0$) for this complex is 8.9 kcal mol$^{-1}$ using the UMP2 method and 50.6 kJ mol$^{-1}$ using the B3LYP method.[43] Several other previous theoretical calculations of the DMS−OH compute similar values using comparable basis sets and methods, such as El Nahas et al.[44] ($D_0 = 37.7$ kJ mol$^{-1}$ at the PMP2/6-311++G(2df,2pd)//MP2/TZ++ level of theory), Gonzalez-Garcia et al.[45] ($D_0 = 37.7$ kJ mol$^{-1}$ at PMP2/6-31G(2d,p) level of theory). These are validated by the experimental observations of Barone et al.[46] and of Hynes et al.,[47] who report bond enthalpies ($\Delta H$) for the DMS−OH complex of 43.1 ± 10.5 kJ mol$^{-1}$ at 298 K and 54.4 ± 13.8 kJ mol$^{-1}$ at 258 K, respectively. Theoretical studies[43] of the reaction mechanism of reaction 9 show that reaction via the DMS−OH complex is an important reaction channel. The binding energy between DMS and $NO_3$ is comparable to that of the DMS−OH complex. Thus, theoretical calculations suggest the existence of an intermediate complex in the reaction mechanism of $NO_3$ + DMS. This result may explain the experimentally determined temperature dependence of the rate constant for of the reaction of $NO_3$ + DMS.

**Acknowledgment.** The authors thank Dr. S. Hashimoto for his help in construction of the apparatus and Mr. S. Enami of Kyoto University for his valuable discussion, respectively. This work was partly supported by a Grant-in-Aid from the Ministry of Education, Science, Sports, and Culture, Japan (No. 16710006).

**Supporting Information Available:** Table and figures of the optimized geometry of the structure calculated at using both the B3LYP/6-311++(3df,3pd) level of theory and the UMP2/6-311++(3df,3pd) level of theory. This material is available free of charge via the Internet at http://pubs.acs.org.

## References and Notes

(1) Cullis, C. F.; Hirschler, M. M. *Atoms. Environ.* **1980**, *14*, 1263.
(2) Andreae, M. O.; Ferek, R. J.; Bermond, F.; Byrd, K. P.; Engstrom, R. T.; Hardin, S.; Houmere, P. D.; Le Marrec, F.; Raemdonck, H.; Chatfield, R. B. *J. Geophys. Res.* **1985**, *90*, 12891.

(3) Bates, T. S.; Lamb, B. K.; Guenther, A.; Dignon, J.; Stoiber, R. E. *J. Atmos. Chem.* **1992**, *14*, 315.
(4) Kettle, A. J.; Andreae, M. O. *J. Geophys. Res.* **2000**, *105*, 2679.
(5) Shon, Z. H.; Davis, D.; Chen, G.; Grodzinsky, G.; Bandy, A.; Thornton, D.; Sandholm, S. Bradshaw, J.; Stickel, R.; Chameides, W.; Kok, G.; Russell, L.; Mauldin, L.; Tanner, D.; Eisele, F. *Atoms. Environ.* **2001**, *35*, 159.
(6) Charlson, R. J.; Lovelock, J. E.; Andreae, M. O.; Warren, S. G. *Nature.* **1987**, *326*, 655.
(7) Houghton, J. T.; Ding, Y.; Griggs, D. J.; Noguer, M.; van der Linden, P. J.; Xiaosu, D.; Maskell, K.; Johnson, C. A. *Climate Change 2001: The Scientific Basis; Contribution of Working Group I to the Third Assessment Report of the Intergovernmental Panel on Climate Change (IPCC)*; Cambridge University Press: New York, 2001; ISBN: 05210 14956 2001.
(8) Hynes, A. J.; Wine, P. H.; Semmes, D. H. *J. Phys. Chem.* **1986**, *90*, 4148.
(9) Barone, S. B.; Turnipseed, A. A.; Ravishankara, A. R. *J. Phys. Chem.* **1996**, *100*, 14694.
(10) Tyndall, G. S.; Ravishankara, A. R. *Int. J. Chem. Kinet.* **1991**, *23*, 483.
(11) Sekušak, S.; Piecuch, P.; Bartlett, R. J.; Cory, M. G. *J. Phys. Chem. A*, **2000**, *104*, 8779.
(12) Cooper, D. J. *J. Atoms. Chem.* **1996**, *25*, 97.
(13) Ravishankara, A. R.; Rudich, Y.; Talukdar, R.; Barone, S. B. *Philos. Trans. R. Res. London. Ser. B*, **1997**, *352*, 171.
(14) Allan, B. J.; McFiggans, G.; Plane, J. M. C.; Coe, H.; McFadyen, G. G. *J. Geophys. Res.* **2000**, *105*, 24191.
(15) Finlayson-Pitts, B. J.; Pitts, J. N. *Chemistry of the Upper and Lower Atmosphere*; Academic Press: San Diego, CA, 1999.
(16) Saiz-Lopez, A.; Plane, J. M. C. *Geophys. Res. Lett.* **2004**, *31*, L04112.
(17) Atkinson, R.; Pitts, J. N.; Aschmann, S. M. *J. Phys. Chem.* **1984**, *88*, 1584.
(18) Tyndall, G. S.; Burrows, J. P.; Schneider, W.; Moortgat, G. K. *Chem. Phys. Lett.* **1986** *130*, 463.
(19) Wallington, T. J.; Atkinson, R.; Winer, A. M.; Pitts, J. N. *J. Phys. Chem.* **1986**, *90*, 4640.
(20) Wallington, T. J.; Atkinson, R.; Winer, A. M.; Pitts, J. N. *J. Phys. Chem.* **1986**, *90*, 5393.
(21) Dlugokencky, E. J.; Howard, C. J. *J. Phys. Chem.* **1988**, *92*, 1188.
(22) Daykin, E. P.; Wine, P. H. *Int. J. Chem. Kinet.* **1990**, *22*, 1083.
(23) Sander, S. P.; Friedl, R. R.; Ravishankara, A. R.; Golden, D. M.; Kolb, C. E.; Kurylo, M. J.; Huie, R. E.; Orkin, V. L.; Molina, M. J.; Moortgat, G. K.; Finlayson-Pitts, B. J. *Chemical Kinetics and Photochemical Data for Use in Stratospheric Modeling: Evaluation 14*; Jet Propulsion Laboratory, Pasadena, CA, 2003. URL for NASA/JPL is http://jpldataeval.jpl.nasa.gov.
(24) Atkinson, R.; Baulch, D. L.; Cox, R. A.; Hampson, R. F., Jr.; Kerr, J. A.; Rossi, M. J.; Troe, J. *IUPAC Summary of Evaluated Kinetic and Photochemical Data for Atmospheric Chemistry*; IUPAC: Cambridge, U.K., 2000; Appendix. URL for IUPAC is http://www.iupac-kinetic.ch.cam.ac.uk.
(25) Jensen, N. R.; Hjorth, J.; Lohse, C.; Skov, H.; Restelll, G. *J. Atmos. Chem.* **1992**, *14*, 95.
(26) Ninomiya, Y.; Hashimoto, S.; Kawasaki, M.; Wallington, T. J. *Int. J. Chem. Kinet.* **2000**, *32*, 125.
(27) Ravishankara, A. R.; Mauldin, R. L. *J. Geophys. Res.* **1986**, *91*, 8709.
(28) Sander, S. P. *J. Phys. Chem.* **1986**, *90*, 4135.
(29) Canosa-Mas, C. E.; Fowles, M.; Houghton, P. J.; Wayne, R. P. *J. Chem. Soc., Faraday Trans. 2* **1987**, *83*, 1465.
(30) Caesar, G. V.; Goldfrank, M. *J. Am. Chem. Soc.* **1946**, *68*, 372.
(31) Nakano, Y.; Ishiwata, T.; Kawasaki, M. *J. Phys. Chem. A* **2004**, *108*, 7785.
(32) Gaussian 03, Revision B.02, Frisch, M. J.; Trucks, G. W.; Schlegel, H. B.; Scuseria, G. E.; Robb, M. A.; Cheeseman, J. R.; Montgomery, J. A., Jr.; Vreven, T.; Kudin, K. N.; Burant, J. C.; Millam, J. M.; Iyengar, S. S.; Tomasi, J.; Barone, V.; Mennucci, B.; Cossi, M.; Scalmani, G.; Rega, N.; Petersson, G. A.; Nakatsuji, H.; Hada, M.; Ehara, M.; Toyota, K.; Fukuda, R.; Hasegawa, J.; Ishida, M.; Nakajima, T.; Honda, Y.; Kitao, O.; Nakai, H.; Klene, M.; Li, X.; Knox, J. E.; Hratchian, H. P.; Cross, J. B.; Bakken, V.; Adamo, C.; Jaramillo, J.; Gomperts, R.; Stratmann, R. E.; Yazyev, O.; Austin, A. J.; Cammi, R.; Pomelli, C.; Ochterski, J. W.; Ayala, P. Y.; Morokuma, K.; Voth, G. A.; Salvador, P.; Dannenberg, J. J.; Zakrzewski, V. G.; Dapprich, S.; Daniels, A. D.; Strain, M. C.; Farkas, O.; Malick, D. K.; Rabuck, A. D.; Raghavachari, K.; Foresman, J. B.; Ortiz, J. V.; Cui, Q.; Baboul, A. G.; Clifford, S.; Cioslowski, J.; Stefanov, B. B.; Liu, G.; Liashenko, A.; Piskorz, P.; Komaromi, I.; Martin, R. L.; Fox, D. J.; Keith, T.; Al-Laham, M. A.; Peng, C. Y.; Nanayakkara, A.; Challacombe, M.; Gill, P. M. W.; Johnson, B.; Chen, W.; Wong, M. W.; Gonzalez, C.; Pople, J. A.; Gaussian, Inc.: Wallingford CT, 2004.
(33) Becke, A. D. *J. Chem. Phys.* **1993**, *98*, 1372.
(34) Lee, C.; Yang, W.; Parr, R. G. *Phys. Rev.* **1988**, *B41*, 785.
(35) Møller, C.; Plesset, M. S. *Phys. Rev.* **1934**, *46*, 618.
(36) Head-Gordan, M.; Pople, J. A.; Frisch, M. J. *Chem. Phys. Lett.* **1988**, *153*, 503.
(37) Head-Gordan, M.; Gordan-Head, T. *Chem. Phys. Lett.* **1994**, *220*, 122.
(38) Becke, A. D. *J. Chem. Phys.* **1993**, *98*, 1372.
(39) Lee, C.; Yang, W.; Parr, R. G. *Phys. Rev.* **1988**, *B41*, 785.
(40) Møller, C.; Plesset, M. S. *Phys. Rev.* **1934**, *46*, 618.
(41) Head-Gordan, M.; Pople, J. A.; Frisch, M. J. *Chem. Phys. Lett.* **1988**, *153*, 503.
(42) Head-Gordan, M.; Gordan-Head, T. *Chem. Phys. Lett.* **1994**, *220*, 122.
(43) Aloisio, S., in press *Chem. Phys.* 2006.
(44) El-Nahas, A. M.; Uchimaru, T.; Masaaki, S.; Tokuhashi, K.; Sekiya, A. *J. Mol. Struct: THEOCHEM* **2005**, *722*, 9.
(45) González-Garcia, N.; González-LaFont, A.; Lluch, J. M. *J. Comput. Chem.* **2005**, *26*, 569.
(46) Barone, S. B.; Turnipseed, A. A.; Ravishankara, A. R. *J. Phys. Chem.* **1996**, *100*, 14694.
(47) Hynes, A. J.; Stoker, R. B.; Pounds, A. J.; McKay, T.; Bradshaw, J. D.; Nicovich, J. M.; Wine, P. H. *J. Phys. Chem.* **1995**, *99*, 16967.